Dehydrocrenatidine extracted from *Picrasma quassioides* induces the apoptosis of nasopharyngeal carcinoma cells through the JNK and ERK signaling pathways

MING-CHANG HSIEH[1,2], YU-SHENG LO[3], YI-CHING CHUANG[3], CHIA-CHIEH LIN[3], HSIN-YU HO[3], MING-JU HSIEH[3-6] and JEN-TSUN LIN[6-8]

[1]School of Medical Laboratory and Biotechnology, Chung Shan Medical University; [2]Department of Clinical Laboratory, Chung Shan Medical University Hospital, Taichung 40201; [3]Oral Cancer Research Center, Changhua Christian Hospital, Changhua 500; [4]Institute of Medicine, Chung Shan Medical University, Taichung 40201; [5]Graduate Institute of Biomedical Sciences, China Medical University, Taichung 404; [6]Post Baccalaureate Medicine, National Chung Hsing University, Taichung 402; [7]Division of Hematology and Oncology, Department of Medicine, Changhua Christian Hospital, Changhua 500; [8]School of Medicine, Chung Shan Medical University, Taichung 40201, Taiwan, R.O.C.

Received March 16, 2021; Accepted June 2, 2021

DOI: 10.3892/or.2021.8117

Abstract. Nasopharyngeal carcinoma (NPC) is an indicator disease in Asia due to its unique geographical and ethnic distribution. Dehydrocrenatidine (DC) is a β-carboline alkaloid abundantly present in *Picrasma quassioides* (D. Don) Benn, a deciduous shrub or small tree native to temperate regions of southern Asia, and β-carboline alkaloids play anti-inflammatory and antiproliferative roles in various cancers. However, the mechanism and function of DC in human NPC cells remain only partially explored. The present study aimed to examine the cytotoxicity and biochemical role of DC in human NPC cells. The MTT method, cell cycle analysis, DAPI determination, Annexin V/PI double staining, and mitochondrial membrane potential examination were performed to evaluate the effects of DC treatment on human NPC cell lines. In addition, western blotting analysis was used to explore the effect of DC on apoptosis and signaling pathways in related proteins. The analysis results confirmed that DC significantly reduced the viability of NPC cell lines in a dose- and time-dependent manner and induced apoptosis through internal and external apoptotic pathways (including cell cycle arrest, altered mitochondrial membrane potential, and activated death receptors). Western blot analysis illustrated that DC's effect on related proteins in the mitogen-activated protein kinase pathway can induce apoptosis by enhancing ERK phosphorylation and inhibiting Janus kinase (JNK) phosphorylation. Notably, DC induced apoptosis by affecting the phosphorylation of JNK and ERK, and DC and inhibitors (SP600125 and U0126) in combination restored the overexpression of p-JNK and p-ERK. To date, this is the first study to confirm the apoptosis pathway induced by DC phosphorylation of p-JNK and p-REK in human NPC. On the basis of evidence obtained from this study, DC targeting the inhibition of NPC cell lines may be a promising future strategy for NPC treatment.

Introduction

The most common malignant tumor of nasopharyngeal epithelial cells is nasopharyngeal carcinoma (NPC) (1). It is relatively rare in the world and has a unique geographical distribution in Asia, particularly in East and Southeast Asia. According to the records of the International Agency for Research on Cancer, approximately 129,000 new cases of nasopharyngeal cancer occurred in 2018, accounting for only 0.7% of all cancers diagnosed in 2018 (2). NPC pathogenesis is closely related to Epstein-Barr virus (EBV) infection, human papillomavirus infection, genetic susceptibility, and consumption of salted fish. Furthermore, cancer-derived EBV DNA circulating in plasma has been identified as a tumor marker for NPC with 96% sensitivity (3,4). The anatomical location of NPC makes it difficult to access for surgery and is highly sensitive to radiation. Therefore, radiotherapy (RT) is the treatment of choice for non-metastatic NPC (5). Intensity-modulated radiation therapy is the most commonly recommended radiation method because of its excellent local control. For locally advanced NPC, concurrent RT and chemo-

Correspondence to: Dr Ming-Ju Hsieh, Oral Cancer Research Center, Changhua Christian Hospital, 135 Nanxiao Street, Changhua County, Changhua 500, Taiwan, R.O.C.
E-mail: 170780@cch.org.tw

Dr Jen-Tsun Lin, Division of Hematology and Oncology, Department of Medicine, Changhua Christian Hospital, 135 Nanxiao Street, Changhua County, Changhua 500, Taiwan, R.O.C.
E-mail: 111227@cch.org.tw

Key words: dehydrocrenatidine, nasopharyngeal cancer, apoptosis, MAPK pathway

therapy is recommended as first-line treatment (6). Studies have indicated that simultaneous chemotherapy and RT may increase treatment-related toxicity and reduce willingness to undergo treatment, which may cause some patients to stop using RT (7). Therefore, providing appropriate treatment guidelines and reducing drug toxicity can further increase the cure rate of cancer.

Natural compounds extracted from plants are used as traditional medicines for treating various diseases, including various cancer types. In addition, natural medicine use has relatively low toxicity. Traditional Chinese pharmacopoeia has used *Picrasma quassioides* (D. Don) Benn (PQ), a deciduous shrub or small tree native to temperate regions of southern Asia, for the treatment of inflammation, microbial infections, and fever. PQ produces various compound types, such as alkaloids (mainly β-carboline and cathinone alkaloids), bitter components, and triterpenoids (8). The β-carboline alkaloids extracted from PQ, which feature anti-inflammatory and antitumor activity, are widely used in medical treatment (9-13).

Dehydrocrenatidine (DC) is a β-carboline alkaloid abundantly present in PQ (14). Zhao *et al* demonstrated that β-carboline alkaloids (the main active ingredient of medicinal plants) exert anti-inflammatory effects through the inhibition of the iNOS pathway (15). The β-carboline enantiomer extracted from PQ was found to decrease cell viability and inhibit the proliferation of various cancer cells, such as liver, cervical, and breast cancer cells (10,14,16,17). Zhao *et al* demonstrated that the analgesic effect of DC may be achieved through the inhibition of neuronal excitability (14). Zhang *et al* showed that the Janus kinase (JAK) inhibitor DC inhibits JAK2 in the tumorigenesis of solid tumors constitutively activated through signal transduction and by transcription activator 3 (18). However, the molecular targeting effect of DC on human NPC cells is unclear. The present study aimed to examine the cytotoxicity and biochemical role of DC in human NPC cells.

Materials and methods

Cell culture. Human NPC cell lines [including NPC-039 and NPC-BM (19)] were provided by Dr Jen-Tsun Lin, Department of Hematology and Oncology, Changhua Christian Hospital. RPMI-2650 head and neck squamous cell line was obtained from Japanese Collection of Research Bioresources Cell Bank (JCRB Cell Bank, Osaka, Japan) cultured in Eagle's Minimum Essential Medium (Gibco BRL; Thermo Fisher Scientific, Inc.) with 10% non-essential amino acids (Gibco BRL; Thermo Fisher Scientific, Inc.) and 10% fetal bovine serum (FBS) (Gibco BRL; Thermo Fisher Scientific, Inc.). NPC cell lines were cultured in RPMI-1640 medium (Gibco BRL; Thermo Fisher Scientific, Inc.) and 10% FBS. All cell lines were cultured under the same conditions (at 37˚C and 5% CO_2 in a humid atmosphere) as described in previous studies (20).

DC treatments. DC (purity ≥98%) was purchased from ChemFaces, and the product was made into a 100 mM stock solution in dimethyl sulfoxide (DMSO) and stored at -20˚C. The final treatment concentration in experiments with DMSO content was consistently less than 0.1%. Various concentrations (0, 25, 50 and 100 μM) of DC were prepared to treat NPC cells in subsequent experiments and were incubated for 24 h.

Cell viability. The effect of DC on cell growth was determined using the MTT method (20). First, NPC-BM, NPC-039 and RPMI-2650 cell lines were seeded on a plate ($1x10^4$ cells/well), treated with various concentrations of DC, and cultured at 37˚C for 24 h. Then, the culture medium was removed, MTT reagent (final concentration of 0.5 mg/ml) was added to each well, and cells were incubated in 5% (v/v) CO_2 at 37˚C for >4 h. After centrifugation, the supernatant was removed. Then, DMSO was carefully added to each well to dissolve formazan crystals for measurement. The absorbance was measured at 595 nm by using an ELISA microplate reader. Each experimental condition was repeated three times, and the data were analyzed for at least three independent experimental results.

Colony formation assays. In a suitable medium, the cell line was seeded on a 6-well cell culture plate at a concentration of $1x10^4$ cells as described in a previous study (21). Then, the cells were evenly distributed and incubated followed by culturing with various DC concentrations. The incubation medium was changed twice a week, and the medium was removed after two weeks. The colonies were further fixed with formalin and stained with 0.5% crystal violet. Finally, a stereo microscope was used to count the total number of colonies and colonies consisting of >50 cells.

Cell cycle analysis. The cells seeded on the plate ($1x10^4$ cells/well) were treated with various DC concentrations and cultured at 37˚C for 24 h as previously described (22). Following the same drug treatment method as specified in previous studies, after the cells were collected through centrifugation and fixed in ethanol, the ethanol was eliminated and the cells were suspended in Muse cell cycle kit reagents and placed in the dark at room temperature. Finally, flow cytometry was used to analyze the cell cycle distribution results.

DAPI staining. The NPC cells ($1x10^4$ cells/well) were grown on glass coverslips and then treated with various DC concentrations for 24 h as described in previous research (20). The method used for cell processing was the same as that in a previous study; according to fixation and permeabilization, the DAPI dye was applied to stain cells in the dark. Nuclear morphological changes associated with apoptosis were evaluated in at least 500 cells. The resulting images were immediately observed through a fluorescence microscope (Leica, Bensheim, Germany).

Annexin V/PI double-staining assay. Cell viability was determined following methods described previously (22). The cells ($1x10^4$ cells/well) were cultured in each well for 12 h and further treated with various DC concentrations for 24 h. These cells were collected and suspended in phosphate-buffered saline (PBS) followed by incubation with reagents contained in the Muse Annexin V and Dead Cell Kit (cat. no. MCH100105; Merck Millipore) in the dark at room temperature. Results were analyzed using Muse Cell Analyzer flow cytometry (Merck Millipore) and the data were analyzed using Muse Cell Soft V1.4.0.0 Analyzer Assays (Merck Millipore).

Mitochondrial membrane potential evaluation. First, the cells were planted in a 6-well plate ($1x10^4$ cells/well) and incubated with various DC concentrations for 24 h as previously described (23). The collected cells were processed under conditions previously studied (23). The obtained cells were added to Muse Mitopotential Assay Kit (cat. no. MCH100110, Merck Millipore) reaction, and the results were analyzed using Muse Cell Analyzer flow cytometry and the data were analyzed using Muse Cell Soft V1.4.0.0 Analyzer Assays (Merck Millipore).

Caspase-3/7 detection and analysis. The analysis was performed as previously described (24). The user guide of the Muse Caspase-3/7 Kit (cat. no. MCH100108, Merck Millipore) describes the caspase-3/7 detection method. After processing the DC, the cells were obtained and stained with the reagent of Muse Caspase-3/7. The experimental results were detected using a flow cytometer and analyzed using Muse Cell Analyzer flow cytometry and the data were analyzed using the Muse Cell Soft V1.4.0.0 Analyzer Assays (Merck Millipore).

Reactive oxygen species (ROS) assay. The user guide of the Muse Oxidative Stress Kit (Cat. No. MCH100111, Merck Millipore) describes the oxidative stress detection method. First, the cells were planted in a 6-well plate ($1x10^4$ cells/well) and incubated with various DC concentrations for 24 h as previously described (23). The collected cells were processed under conditions previously studied (23). The obtained cells were added to the Muse Oxidative Stress working solution reagent reaction at 37˚C for 30 min, and the results were analyzed using Muse Cell Analyzer flow cytometry and the data were analyzed using the Muse Cell Soft V1.4.0.0 Analyzer Assays (Merck Millipore).

Protein extraction and western blot analysis. NPC cell lines (NPC-039 and NPC-BM) were inoculated into 6-well plates and cultured for 12 h; various DC concentrations were added to each well, and the plate was incubated in an incubator at 37˚C for 24 h. Then, the cells were washed with PBS, mixed with an inhibitor reagent, and lysed as described in a previous study (20). BCA protein assay (Pierce; Thermo Fisher Scientific, Inc.) was used to quantify the proteins of the supernatant. All samples were analyzed through sodium dodecyl sulfate polyacrylamide 10% or 12.5% gel electrophoresis, and the separated proteins from the gel were transferred to the PVDF membrane surface (EMD Millipore). The PVDF membrane was reacted with 5% skimmed milk in TBST for 1 h. For analysis, the primary antibody was used, which was described by the antibody manufacturer [from Cell Signaling Technology, Inc. (CST), 1:1,000 dilution] as containing cell cycle related-proteins [cyclin A (cat. no. #4656; 55 kDa), cyclin B (cat. no. #12231; 55 kDa), cyclin D3 (cat. no. #2936; 31 kDa), cyclin-dependent kinase (CDK)4 (cat. no. #12790; 30 kDa), CDK6 (cat. no. #3136; 36 kDa), phosphorylated (p)-cdc2 (cat. no. #4539; 34 kDa), Myt1 (cat. no. #4282; 60-70 kDa), p-WEE1 (cat. no. #4910; 95 kDa), and p-Rb (cat. no. #8516; 110 kDa) (cat. no. #9301; 110 kDa)] death receptor pathway-related proteins (FADD (cat. no. #2782; 28 kDa), TNF-R1 (cat. no. #3736; 55 kDa), DcR2 (cat. no. #8049; 45-60 kDa), cleaved RIP (cat. no. #3493; 78 kDa), and DR5 (cat. no. #8074; 40, 48 kDa)), apoptosis-related proteins (cleaved PARP (cat. no. #9542; 89, 116 kDa), cleaved caspase-3 (cat. no. #9664; 17, 19 kDa), cleaved caspase-8 (cat. no. #9496; 41, 43 kDa), cleaved caspase-9 (cat. no. #52873; 37 kDa), Bax (cat. no. #5023; 20 kDa), Bak (cat. no. #12105; 25 kDa), t-Bid (cat. no. #2002; 15, 22 kDa), Bcl-xL (cat. no. #2764; 30 kDa), and Bcl-2 (cat. no. #4223; 26 kDa), MAPK pathway-related proteins (AKT (cat. no. #4685, 60 kDa), ERK1/2 (cat. no. #4695; 42, 44 kDa), p38 (cat. no. #8690; 40 kDa), JNK1/2 (cat. no. #9252; 46, 54 kDa), p-AKT (cat. no. #4060; 60 kDa), p-ERK1/2 (cat. no. #4370; 42, 44 kDa), p-p38 (cat. no. #4511; 43 kDa), and p-JNK1/2 (cat. no. #4668; 46, 54 kDa)), and β-actin (1:5000 dilution; cat. no. # NB600-501; 42 kDa; Novus Biologicals). Finally, after washing with TBST, the PVDF membrane was incubated with secondary anti-rabbit IgG (anti-rabbit IgG, #7074, 1:3,000) or anti-mouse IgG (anti-mouse IgG, #7076, 1:3,000) (Cell Signaling Technology, Inc.) attached to HRP for 1 h. The western blot was observed using a chemiluminescence HRP substrate (Millipore), and the photographic images observed by ImageQuant LAS 4000 mini (GE Healthcare, USA) and relative density quantitated by ImageJ 1.47 version software (National Institutes of Health).

Statistical analysis. For the statistical analysis, GraphPad Prism software (GraphPad Software, Inc.) was used, as in a previous study (23). Statistical analysis of at least three independent experimental results was performed, and the calculated values are presented as mean ± standard deviation. Statistical analysis methods used included ANOVA and Tukey's post hoc test. A P-value <0.05 represented a valid significant difference.

Results

DC causes cytotoxicity by inhibiting the survival and proliferation of human NPC cell lines. We investigated the cell viability of the human NPC cell lines (including NPC-039 and NPC-BM) and human head and neck squamous cell carcinoma (RPMI-2650). These cells were treated with various DC concentrations (0, 25, 50, and 100 μM) for 24, 48, and 72 h to measure DC cytotoxicity. MTT analysis revealed that the cell viability of these cell lines was reduced by DC in a dose- and time-dependent manner ($P<0.05$; Fig. 1A-C). The MTT analysis showed that DC induced approximately 40% of death by apoptosis in the NPC-BM and RPMI-2650 cell lines and approximately 23% in the NPC-039 cell line at the highest concentration. These results suggest that the nasopharyngeal cancer cell lines were not resistant to the action of DC, and nasopharyngeal cancer cells are also sensitive to the action of DC. Moreover, to analyze the effect of DC against cell proliferation in human NPC cell lines, the colony formation results were studied to determine the effect of DC on both cell lines during long-term treatment. Fig. 1D and E show that a DC concentration of 25 μM significantly inhibited the colony forming ability of both cell lines. Therefore, DC inhibited the survival and proliferation of NPC-039, NPC-BM and RPMI-2650 cell lines.

DC induces cell cycle arrest and apoptosis of human NPC cells. We explored whether various DC concentrations (0, 25, 50, and 100 μM) affect cell viability and apoptosis within

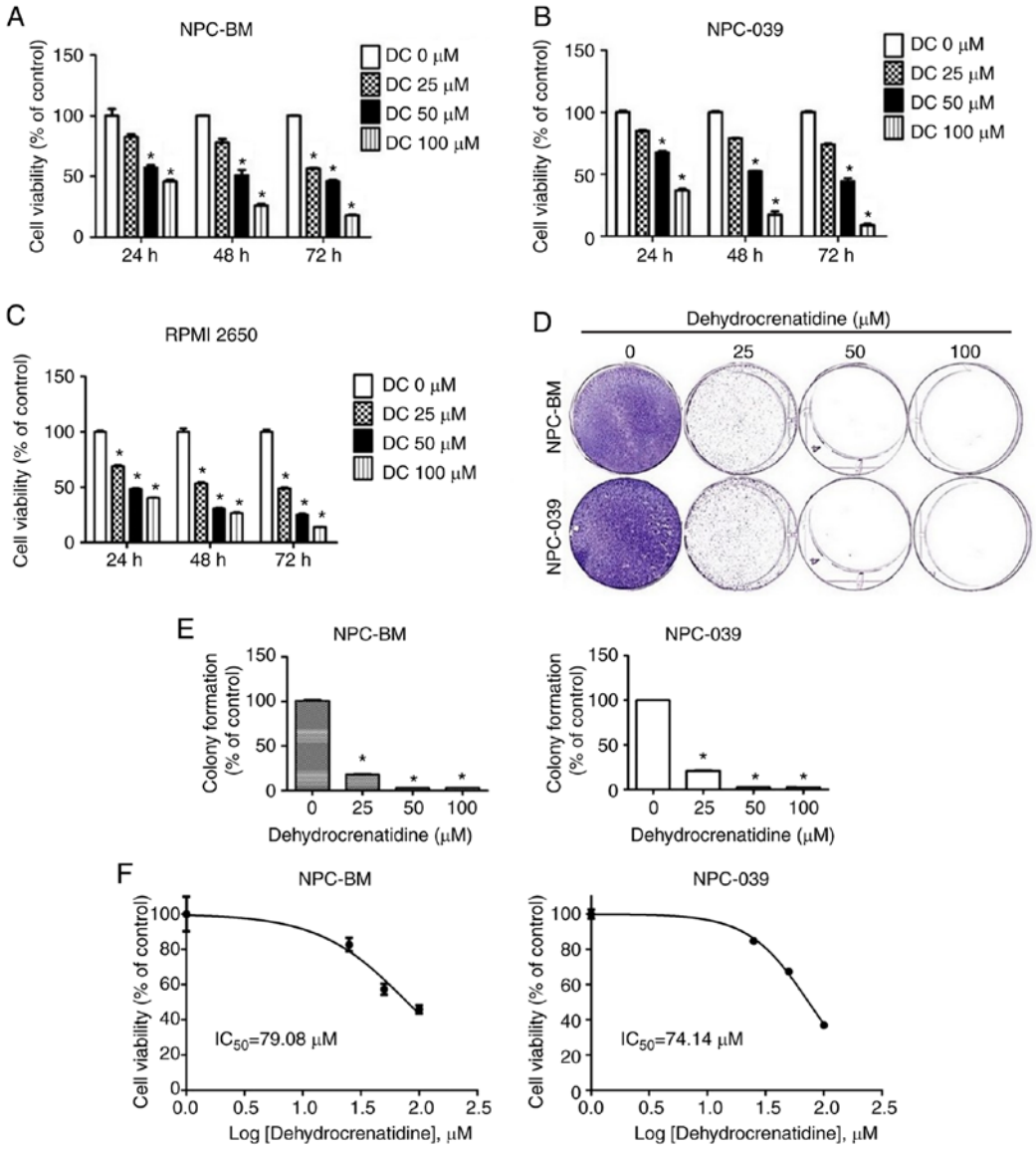

Figure 1. DC causes cytotoxicity in human NPC cells. (A-C) Human NPC cell lines (including NPC-039 and NPC-BM) and RPMI-2650 were individually treated with various concentrations (0, 25, 50, and 100 μM) of DC for 24, 48, and 72 h. Cell viability was analyzed using MTT analysis. (D and E) In the colony formation assay, NPC-039 and NPC-BM cell lines were evenly distributed and incubated and then cultured with various DC concentrations (0, 25, 50, and 100 μM). The incubation medium was changed twice a week, and the medium was removed after 2 weeks. (F) The IC_{50} values of NPC cells after treatment with DC. *P<0.05 vs. the control group. NPC, nasopharyngeal carcinoma; DC, dehydrocrenatidine; IC_{50}, half maximal inhibitory concentration.

24 h and analyzed the cell cycle distribution of NPC-039 and NPC-BM cell lines by using PI staining and flow cytometry. Fig. 2A and B demonstrate that in both cell lines, DC at 100 μM resulted in a significant increase in the sub-G1 phase and decreased the number of cells in the G0/G1 phase for both cell lines (P<0.05). We understand that sub-G1 and G2/M phases block cell cycle binding of the cyclin-CDK complex induced by DC. We further explored whether DC regulates the expression of G2/M cell cycle regulators and then checked the level of G2/M cell cycle regulators by using western blot analysis. As shown in Fig. 2C and D, in both cell lines, the expression levels of cyclin A and B were decreased (DC, 100 μM), and regulatory proteins p-cdc2 (Tyr15), Myt1, and p-WEE1 (Ser642) were decreased at high DC concentrations. Furthermore, we investigated DC regulation of the expression of the G0/G1 cell cycle regulator and analyzed the level of the G0/G1 cell cycle regulator. Fig. 2C and D show that the expression levels of cyclin D3, CDK4, and CDK6 were decreased after NPC-039 and NPC-BM cells were treated with a high DC concentration, thereby reducing the effect of regulatory protein p-Rb. Next, we determined whether the growth inhibitory effect of the NPC-BM and NPC-039 cell lines treated with DC leads to apoptosis. After DAPI staining, DC-treated NPC-BM and NPC-039 cell lines were examined using a fluorescence microscope. Cells treated with DC showed significant morphological changes compared with control cells, leading to nuclear bleb formation in both cell lines (Fig. 3A). Next, we examined whether NPC-BM and NPC-039 cell lines treated with DC showed a significant increase in dose-dependent DNA condensation folding compared with the control (Fig. 3B; P<0.05). To further clarify whether apoptosis was affected by treating NPC-BM and NPC-039 cell lines with DC, we used Annexin V/PI double staining to check cell morphology and measured the results with flow cytometry. Notably, compared

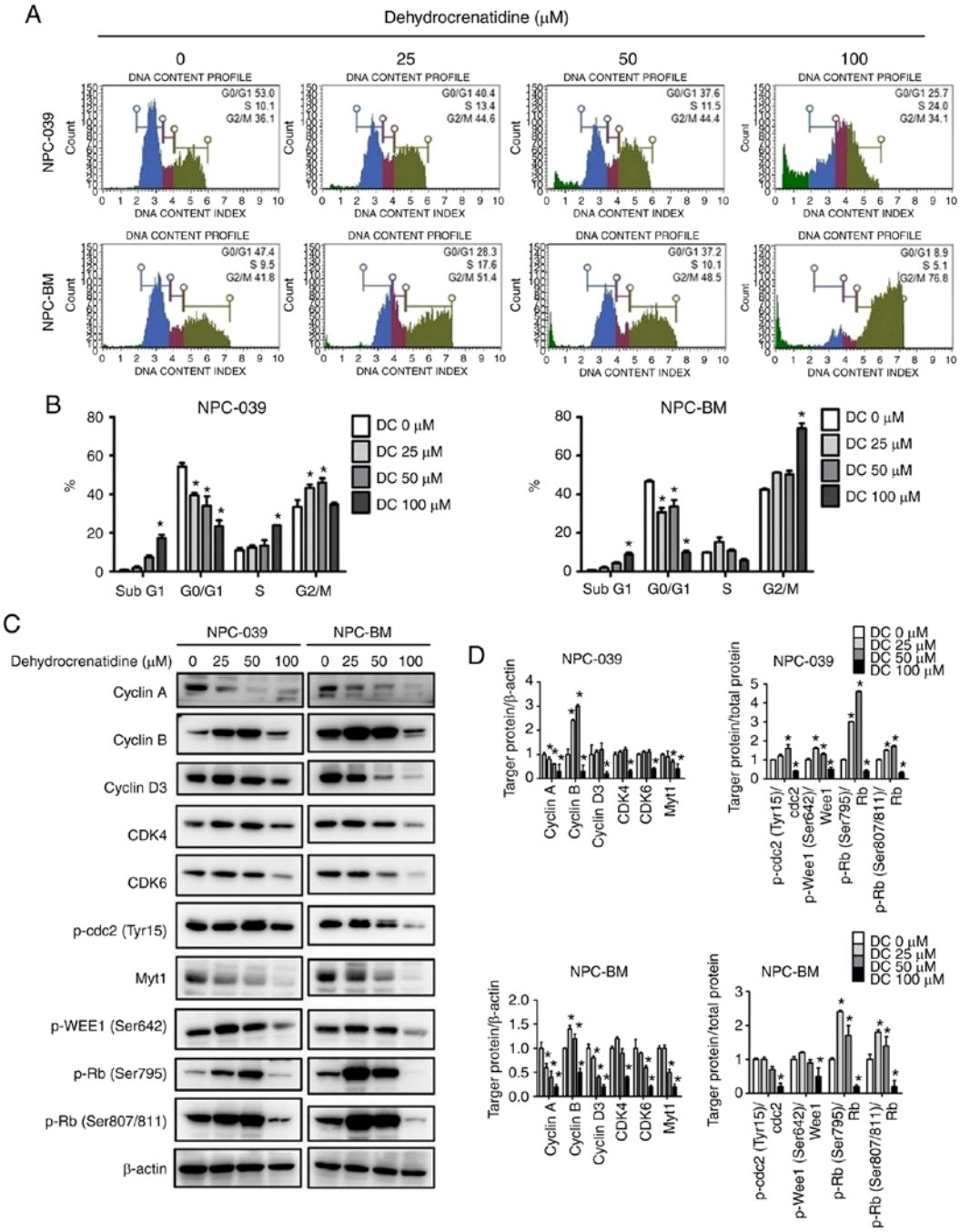

Figure 2. DC-mediated cell cycle arrest in human NPC cell lines (including NPC-039 and NPC-BM). (A) NPC-039 and NPC-BM cell lines were treated with DC (0, 25, 50, and 100 μM) to measure and predict the phase distribution of the cell cycle (G0/G1, S, and G2/M) by using flow cytometry. (B) Distribution of cell cycle phases in the NPC-039 and NPC-BM cell lines was detected and compared with the control group. (C and D) Western blotting for the determination of cell cycle marker-related proteins showed the levels of cyclin A, cyclin B, cyclin D3, CDK4, CDK6, p-cdc2, Myt1, p-WEE1, and p-Rb. β-actin was used as an internal standard for protein expression, and the results of protein levels were normalized to β-actin for quantification. *P<0.05 vs. the control group. NPC, nasopharyngeal carcinoma; DC, dehydrocrenatidine; CDK, cyclin-dependent kinase; Myt1, myelin transcription factor 1; WEE1, WEE1 G2 checkpoint kinase; Rb, retinoblastoma protein; p-, phosphorylated.

with the control, the apoptotic rate of DC-treated cells was significantly increased (DC, 50 and 100 μM) (Fig. 3C and D; P<0.05). These results confirmed that DC can reduce the viability of human NPC cell lines.

Apoptosis of human NPC cells induced by DC is related to the extrinsic and intrinsic apoptosis pathway. To determine the apoptotic mechanism in NPC-039 and NPC-BM cells induced by DC, the results were analyzed using Muse's flow cytometer and software. Treatments to increase the DC concentration in both cell lines significantly enhanced the depolarization of the mitochondrial membrane compared with the untreated cells. Furthermore, DC (50 and 100 μM) significantly increased depolarized cells in a dose-dependent manner (Fig. 4A; P<0.05). In addition, we conducted a study on the role of DC in the death receptor pathway of NPC-039 and NPC-BM through western blot analysis. As illustrated in Fig. 4B and C, western blot analysis revealed that human NPC cell lines treated with

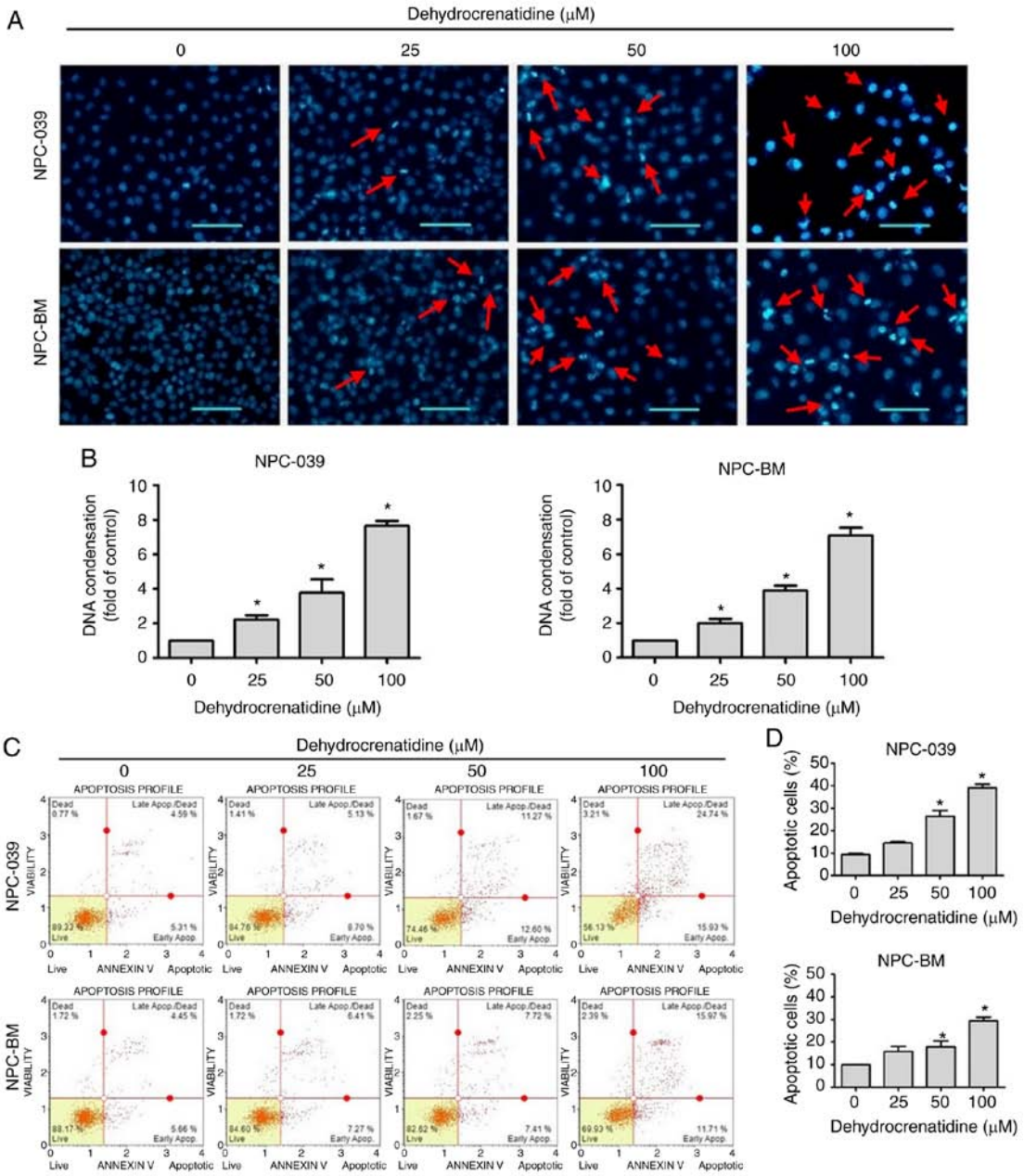

Figure 3. DC induces cell apoptosis in human NPC cell lines (including NPC-039 and NPC-BM). (A) DAPI staining was used to analyze the level of nuclear counterstaining. The characteristic morphology of blebbing nuclei was detected by using fluorescence microscopy. Nuclei condensation and fragmentation are indicated by red arrows. (B) The results of A were quantified by assessing the total cell nuclei with DNA condensation. (C) Annexin V/PI staining was used to reveal DC-induced apoptosis. (D) The percentage distribution of apoptotic cells including early and late apoptotic states. *P<0.05 vs. the control group. NPC, nasopharyngeal carcinoma; DC, dehydrocrenatidine.

DC exhibited increased protein expression levels of FADD, TNF-R1, DcR2, cleaved RIP, and DR5 (P<0.05).

DC induces apoptosis of human NPC cells through the cell signaling pathway in the induction of the extrinsic and intrinsic apoptosis pathway. The cell signal transduction pathway of DC in the activation of the extrinsic and intrinsic apoptotic pathways was evaluated. To investigate the role of caspase in the process of DC-induced apoptosis, we tested the effect of DC-activated caspase using flow cytometry and western blot assay. Fig. 5A and B demonstrate that DC (50 and 100 μM) treatment increased the cell levels in caspase-3 and caspase-7 in both cell lines and achieved a significant dose-dependent increase in fold activation expression compared with the control (P<0.05). The expression levels of cleaved caspase-3, -8, and -9 and cleaved PARP were all significantly enhanced in human NPC cells treated with DC at high concentrations based on western blot analysis (Fig. 5C and D; P<0.05). Thus, DC can significantly provoke caspase activation in human NPC cells. The related expression levels of the apoptosis-regulating proteins Bax, Bak, and t-Bid (truncated BID, cleaved at Asp60 by caspase-8 during Fas signaling) were significantly increased in both cell lines, whereas Bcl-xL expression was decreased in a dose-dependent manner. Bcl-2 expression changes were not seen at all concentrations and for both cell lines (Fig. 5E and F;

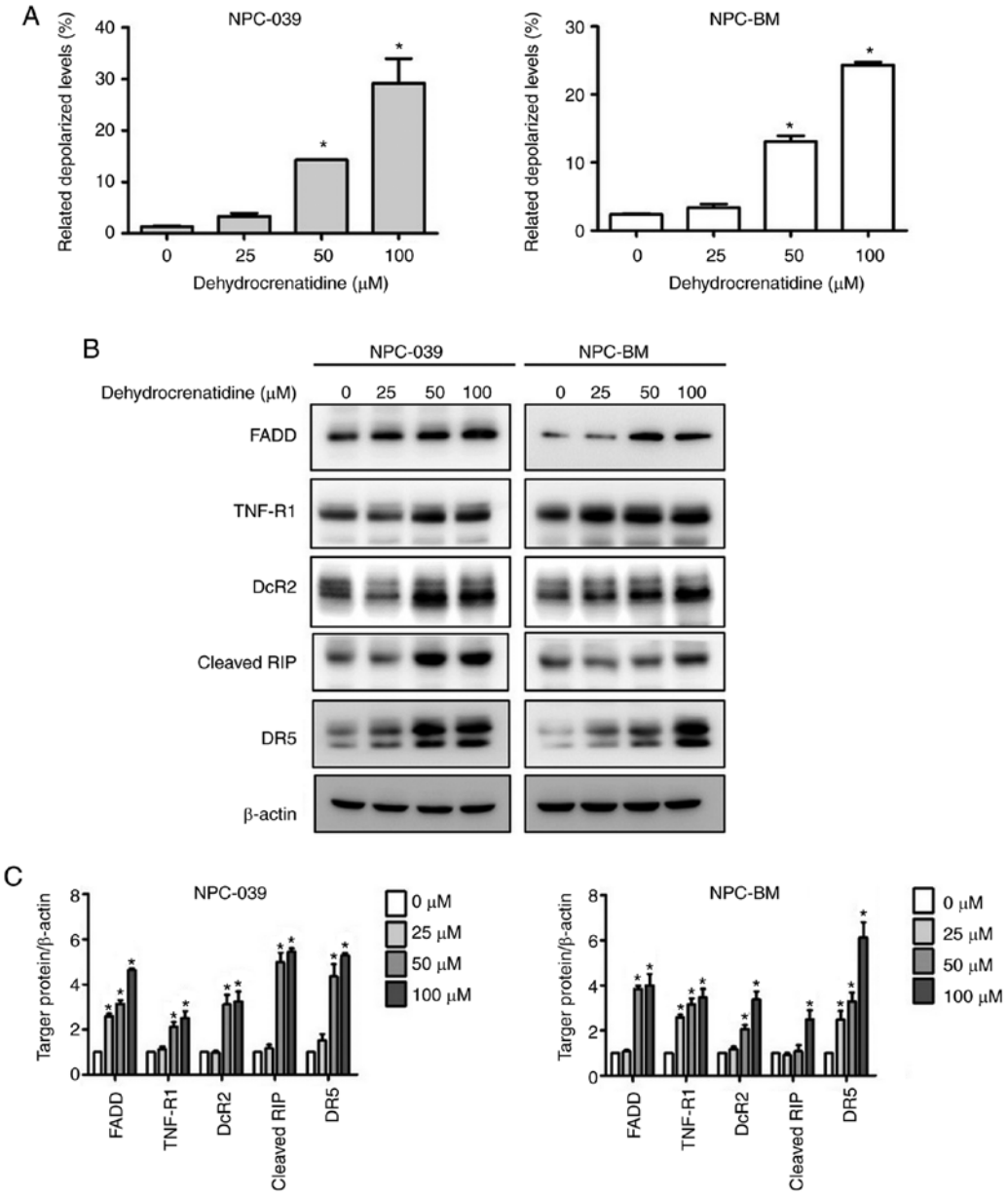

Figure 4. DC treatment leads to the apoptosis of human NPC cell lines (including NPC-039 and NPC-BM) through the mitochondrial and death receptor pathways. (A) Mitochondrial membrane potential was analyzed after treatment with DC (0, 25, 50, and 100 μM) by using the Muse Cell Analyzer. Quantitative results were analyzed using Muse Cell software and compared with the control group. (B and C) Protein levels of the Fas pathway and the TNF pathway including FADD, TNF-R1, DcR2, cleaved-RIP, and DR5 were detected by western blotting. β-actin was used as an internal standard for protein expression, and the results of protein levels were normalized to β-actin for quantification. *P<0.05 vs. the control group. NPC, nasopharyngeal carcinoma; DC, dehydrocrenatidine; FADD, FAS-associated death domain protein; TNF-R1, tumor necrosis factor receptor 1; DcR2, decoy receptor 2; RIP, ribosome-inactivating protein; DR5, death receptor 5.

P<0.05). The expression levels of cleaved caspase-3, -8, and -9 and cleaved PARP were significantly decreased in human NPC cells following combined treatment with DC and Z-VAD-FMK (caspase inhibitor) based on western blot analysis (Fig. 5G and H).

DC regulates the protein expression of the MAPK pathway in human NPC cells. To clarify the role of protein expression levels in the MAPK pathway and to confirm the mechanism related to DC-mediated apoptosis, western blot analysis was used. In particular, western blot analysis revealed that the DC-treated human NPC cells exhibited upregulated phosphorylated (p)-AKT and p-ERK1/2 and downregulated p-JNK1/2 (Fig. 6A and B; P<0.05). In addition, p-p38 activation remained unchanged after treatment with DC in both cell lines, and DC treatment increased the expression of p-AKT and p-ERK1/2 in both cell lines and decreased the expression of p-JNK1/2. To explore whether the MAPK pathway directly mediates DC-induced apoptosis, we pretreated human NPC cells with AKT inhibitor (LY294002), ERK inhibitor (U0126), and JNK1/2 inhibitor (SP600125) for 24 h before DC treatment. The results in Fig. 6E-H demonstrate that the co-treatment with the ERK1/2 inhibitor resulted in a significantly higher reduction of apoptosis-related proteins in both cell lines as compared to the DC treatment alone (P<0.05), whereas the co-treatment with JNK1/2 inhibitor resulted in a

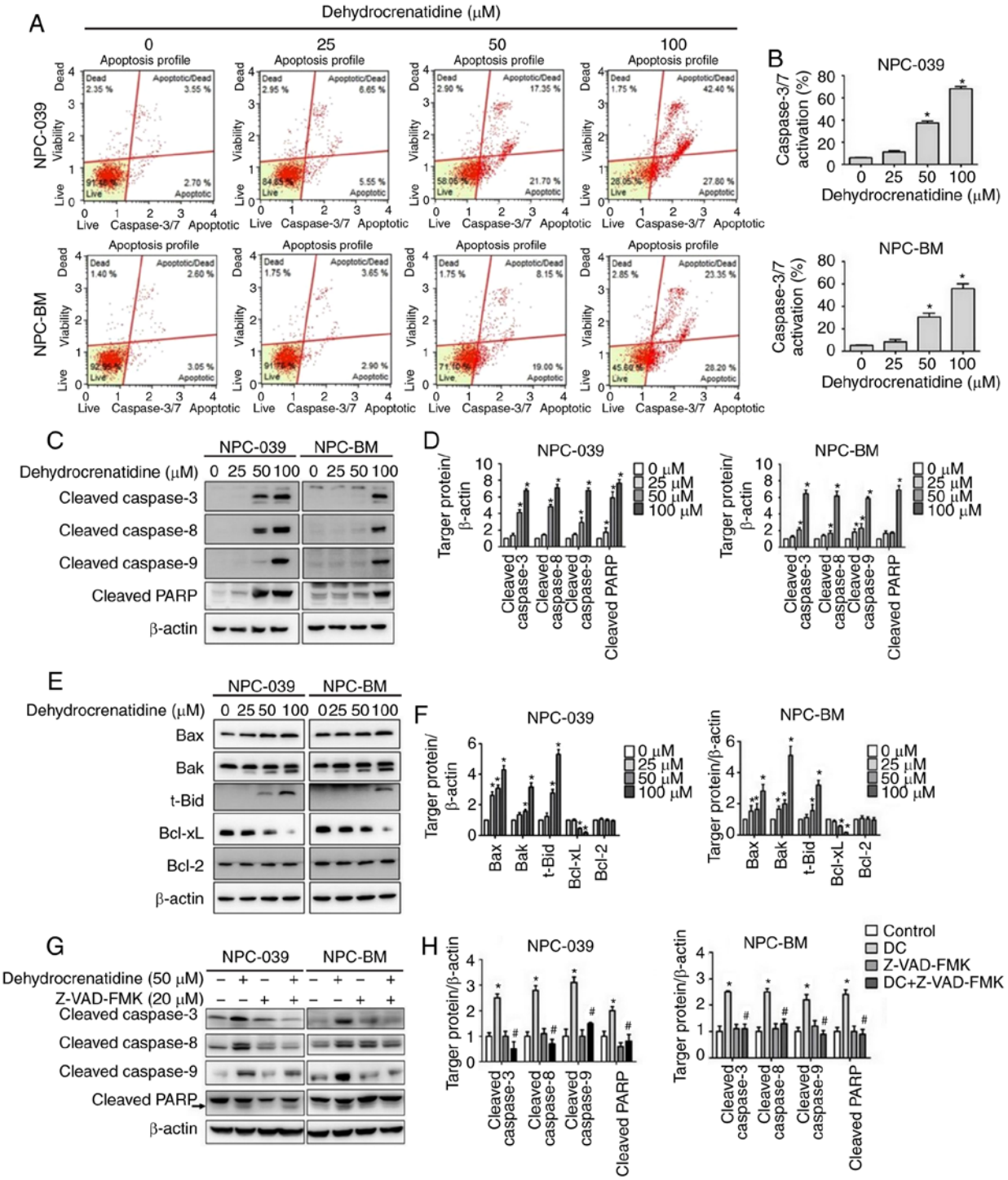

Figure 5. DC promotes apoptosis through the regulation of apoptosis-related proteins in human NPC cell lines (including NPC-039 and NPC-BM) through extrinsic and intrinsic caspase cell signaling pathways. (A and B) After treatment of NPC-039 and NPC-BM cell lines for 24 h with DC, caspase-3/7 was detected using the Muse caspase-3/7 kit. The level of caspase-3/7 activation was quantitatively analyzed in the treatment group and compared with the control group. (C and D) The activated form of apoptosis proteins was detected through western blotting, including cleaved caspase-3, -8, and -9 and cleaved PARP proteins. (E and F) Expression levels of related proteins, including Bax, Bak, t-Bid, Bcl-xL, and Bcl-2 proteins, were determined and quantified through Western blotting. *P<0.05 vs. the control group. (G and H) Cell lines were pre-treated with Z-VAD-FMK (20 μM) for 1 h, then with treated DC (50 μM) for 24 h. The activated form of apoptosis proteins was detected through western blotting, including cleaved caspase-3, -8, and -9 and cleaved PARP proteins. Protein levels were determined through densitometry, with β-actin as an internal standard for protein expression. Results of all protein levels were normalized to β-actin for quantification compared with the control, *P<0.05 vs. the control group; #P<0.05 vs. DC treatment alone group. NPC, nasopharyngeal carcinoma; DC, dehydrocrenatidine; Bax, BCL2 associated X, apoptosis regulator; Bak, BCL2 antagonist/killer 1; Bid, BH3-interacting domain death agonist; Bcl-xL, B-cell lymphoma-extra large; Bcl-2, B-cell lymphoma 2; PARP, poly(ADP-ribose) polymerase.

significantly higher induction of apoptosis-related proteins in both cells as compared to the DC treatment alone (P<0.05). Notably, Fig. 6C and D illustrate that in the presence of an AKT inhibitor, the expression of apoptosis-related proteins of human NPC cells treated with DC remained unaffected compared with treatment with DC alone (P<0.05).

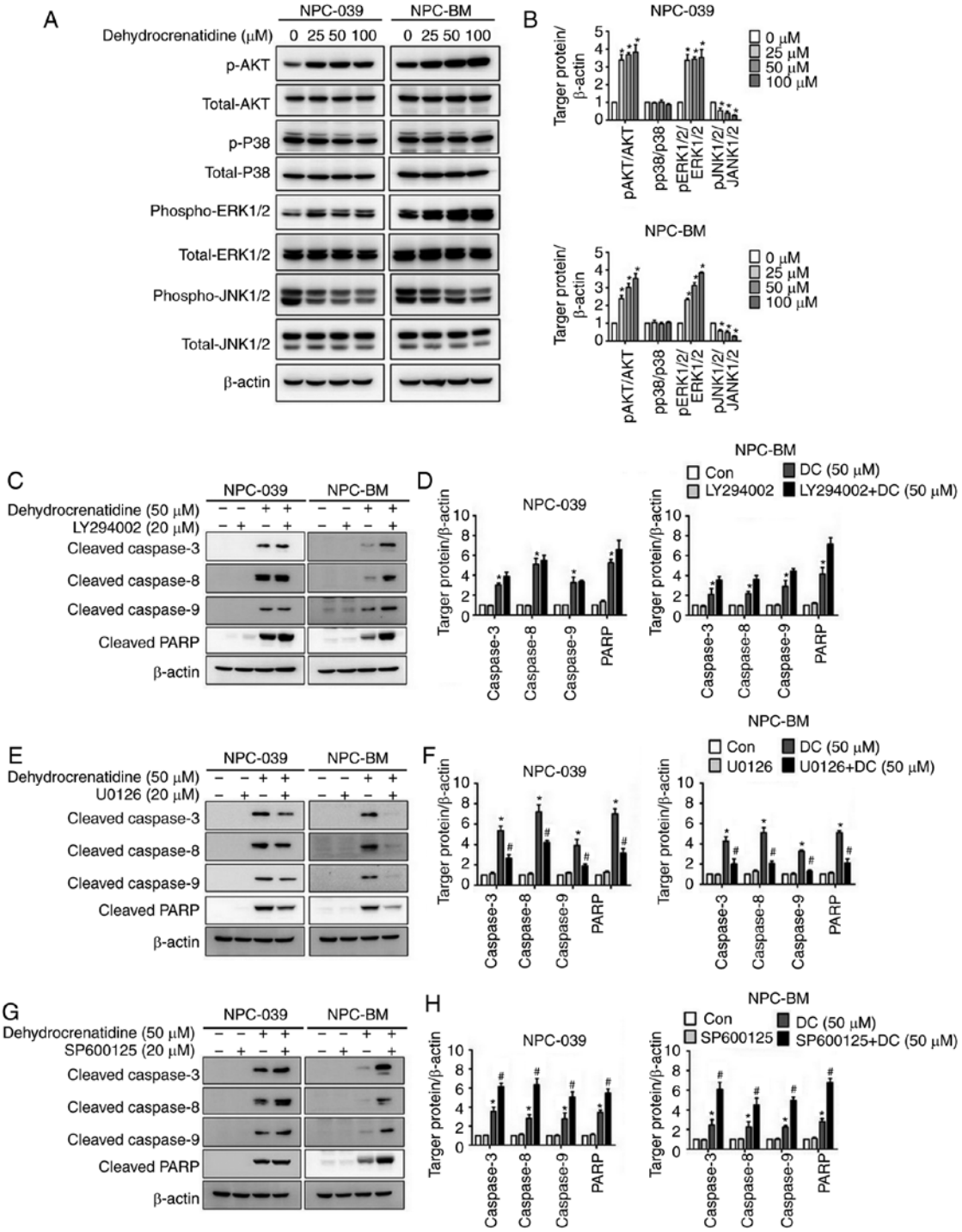

Figure 6. DC regulates the protein expression of the MAPK pathway in human NPC cell lines (including NPC-039 and NPC-BM). (A) Analysis and quantification of expression levels of AKT, p38, ERK1/2, and JNK1/2 proteins through western blotting. (B) Protein levels were analyzed through densitometry; β-actin was used as an internal standard for protein expression, and all proteins were normalized to β-actin. *P<0.05 vs. the control group. (C-H) NPC-039 and NPC-BM cell lines were pretreated with each MAPK inhibitor, including AKT inhibitor (LY294002), ERK1/2 inhibitor (U0126), and JNK1/2 inhibitor (SP600125), for 1 h and then cotreated with or without DC for 23 h. Analysis and quantitative regulation of protein expression, including cleaved caspase-3, -8, and -9 and cleaved PARP protein, through western blotting. Protein levels were determined through densitometry, with β-actin as an internal standard for protein expression. Results of all protein levels were normalized to β-actin for quantification compared with control, *P<0.05 vs. the control group; #P<0.05 vs. DC treatment alone group. NPC, nasopharyngeal carcinoma; DC, dehydrocrenatidine; PARP, poly(ADP-ribose) polymerase; p-, phosphorylated; AKT, protein kinase B (PKB); p38, p38 mitogen-activated protein kinases; ERK, extracellular signal-regulated kinases; JNK, c-Jun N-terminal kinase.

Discussion

Nasopharyngeal carcinoma (NPC) is one of the five main head and neck malignancies that develop in the lining of the nasopharyngeal epithelium. However, the causes of NPC and treatment strategies are different from those of other head and neck cancers (25). The prognosis of NPC patients has considerably improved with the combined use of magnetic resonance imaging, intensity-modulated radiotherapy (RT), and concurrent chemoradiation (26,27). NPC is highly

sensitive to RT and chemotherapy. Due to local recurrence and distant metastasis, prognosis is poor in approximately 15-60% of cases (25). Approximately 30% of NPC patients present recurrence or distant metastasis, resulting in poor treatment of these patients (28). Head and neck squamous cell carcinoma (HNSCC) arises from the mucosal epithelium of the oral cavity, nasopharynx, oropharynx, hypopharynx and larynx. However, it is difficult to obtain important NPC cell lines from research institutions. Only RPMI-2650 head and neck squamous cell carcinoma was obtained from the Japanese Collection of Research Bioresources Cell Bank.

The compounds of natural plants or traditional Chinese medicine have anticancer effects. For example, β-carboline belongs to the class of indole alkaloids. These compounds have attracted much attention owing to their various biological activities. In particular, these compounds have been shown to insert themselves into DNA and consequently inhibit CDK, topoisomerase, and monoamine oxidase (29). In addition, β-carboline derivatives exhibit a wide range of pharmacological properties, leading to cytotoxic and antiproliferative effects on other cancer cells, including fibrosarcoma, prostate cancer, lung cancer, melanoma, colorectal cancer, liver cancer, breast cancer, and cervical cancer (30-32). The β-carboline alkaloid derivative dehydrocrenatidine (DC) is predominantly isolated from *Picrasma quassioides* (D. Don) Benn (PQ). Studies have shown that the toxic properties of β-carboline alkaloid derivatives in PQ lead to apoptosis in HepG2 cells (8). Our study revealed that DC cytotoxicity in NPC cell lines was dose- and time-dependent.

The cell cycle is a conservative biological mechanism that controls the growth, development, and differentiation of cells. The cell cycle is mainly adjusted by the cyclin-CDK complex, checkpoint kinase, and CDK inhibitor. Cell cycle disorder is a sign of transformation of normal cells into tumor cells (33). Cyclin A is particularly crucial in cyclins because it participates in the S phase and mitosis, which are related to CDC2 (also known as CDK1) and CDK2; moreover, its expression is increased in many tumors (34). Cyclin A/CDK1 kinase is a factor that triggers mitosis. Vigneron *et al* confirmed that Bora phosphorylation of cyclin A/cdk1 is both necessary and sufficient for mitosis formation (35). The nuclear translocation of cyclin B plays a crucial role in promoting mitosis. The cyclin B/CDK1 complex controls the G2-M phase transition and is essential for initiating mitosis in patients with breast cancer (36). During G2, CDK1 bind to cyclin B mainly through the activation of the complex, which requires cdc25c phosphatase to dephosphorylate cdc2 at the Tyr15 site. Furthermore, cyclin B/CDK1 remains inactivated by WEE1/Myt1-dependent phosphorylation of Tyr15 of cdk1 (37-39). Mota *et al* demonstrated that harmine is a β-carboline alkaloid, which was confirmed to be a specific inhibitor of CDK1/cyclin B and CDK2/cyclin A, which may explain the significant reduction of cells in the S phase and cell cycle arrest in the G2/M phase (40). Notably, in our study, DC induced G2/M blockage of NPC-039 and NPC-BM cell apoptosis by reducing the expression of cyclin A and B and phosphorylated cdc2. However, DC was found to directly lead to the reduction of phosphorylated WEE1 and Myt1 proteins. In the G1 phase, CDK4/6-cyclin D initiates cell cycle progression through RB phosphorylation and chelation of p21 and p27 to release CDK2-cyclin E complex and promote CDK2 kinase activity (33). The aforementioned kinase complexes can phosphorylate RB1 together to release E2F to mediate the transition to the S phase (41). As demonstrated by Ahmad *et al*, β-carboline alkaloids that inhibit G0/G1 transition in cancer cells are believed to inhibit cyclin D1/D3 and reduce CDK4, CDK6, and cyclin E expression in HeLa cells (42). Similarly, our study revealed that DC induced apoptosis by reducing the expression of complex CDK4/6-cyclin D3 protein, thereby inhibiting the expression of RB phosphorylation. Consistent with our results, Cao *et al* indicated that β-carboline alkaloid derivatives and harmine altered the cell cycle distribution by reducing the ratio of cells in the G0/G1 and increasing the ratio in the S and G2/M phases (43). Further mechanistic studies by Abdelsalam *et al* showed that β-carboline alkaloid derivatives can trigger sub-G1 upregulation and cause MDA-MB435 cell cycle arrest (44). In particular, our results showed that DC induced the number of cells in the sub-G1 phase and led to apoptosis. In this study, it was found that DC inhibited the expression of cell cycle check point proteins. However, this was only evident at 100 μM, under which condition the cells barely survived. To note, when treated with DC at 25 and 50 μM, some proteins (including cyclin B, cyclinD3, p-WEE1 and p-Rb) were upregulated in the two cell lines. We hypothesize that this situation was due to cell cycle arrest at different stages of the cell cycle when the cells were treated with low concentrations (25 or 50 μM) of DC at the same time point, resulting in different expression of cell cycle regulatory proteins. This situation lacked consistency across doses, cell lines and time points.

Apoptosis is the main type of cell death that occurs when DNA repair is irreversible and includes external and internal pathways. According to the present data, DNA damage was induced after DC treatment in the NPC cell lines. The extrinsic pathway is mediated by a subgroup of the tumor necrosis factor receptor (TNFR) superfamily, including TNFR, Fas, and TRAIL (45,46). TRAIL induces apoptosis through interaction with its receptors to induce membrane protein receptors, including DR4, DR5, DcR1, DcR2, and osteoprotegerin (47,48). The apoptotic signal transduction mechanism of TNFR1 is similar to Fas, mainly through the combination of a complex (FADD, caspase-8 and RIP cleavage), which are essential for the apoptotic signal transduction of Fas and TNF-R1 (49,50). However, FADD, TNF-R1, DcR2, cleaved RIP, and DR5 were increased in DC-induced apoptosis, a similar finding as in other studies (51-53). The Bcl-2 family proteins play a key role in adjusting the mitochondrial pathway, with particular effect on the antiapoptotic members (Bcl-2 and Bcl-xL) and proapoptotic molecules (Bax, Bak, Bad, and BH3 domains). However, these proteins are connected to the mitochondrial pathway (t-Bid, Bim, Puma, and Noxa) through the death receptor pathway (54,55). Weber indicated that some traditional Chinese medicine compounds whose therapeutic mechanisms are relatively well characterized kill tumor cells through apoptosis induction (55). The β-carboline derivative, harmine, significantly increased the level of active proteins, including caspase-3, -8, and -9, PARP, and Bax, and reduces Bcl-xL expression in different cancers (56-59). The present results showed that DC significantly enhanced the expression of proapoptotic regulatory proteins, including Bax, Bak, and t-Bid, and reduced the expression of antiapoptotic factor protein Bcl-xL. DC increased the expression of caspase-3, -8, and -9 and PARP protein in a dose-dependent manner and

promoted cell apoptosis in NPC-039 and NPC-BM cells. Thus, DC triggers apoptosis through the activation of the caspase pathway and induces the expression of proapoptotic and anti-apoptotic proteins.

The MAPK signaling pathway regulates various biological processes through various cellular mechanisms, including the main proapoptotic and antiapoptotic mechanisms regulated by MAPK (60,61). Studies have shown that compounds of traditional herbal medicines induce apoptosis in different cancers through the JNK/ERK/MAPK signaling pathway (62,63). Lee *et al* demonstrated that PFHxS activation at different times increased the activation of ERK1/2, JNK, and p38 MAPK. Notably, ERK inhibitors significantly reduced apoptosis, whereas JNK inhibitors increased apoptosis (64). Our results showed that the co-treatment with ERK1/2 inhibitor resulted in a significantly higher reduction of apoptosis-related proteins in both cell lines as compared to the DC treatment alone, whereas the co-treatment with JNK1/2 inhibitor resulted in a significantly higher induction of apoptosis-related proteins in both cells as compared to the DC treatment alone. Thus, DC-mediated MAPK signal transduction induced apoptosis of human NPC cells. Given that radiation therapy and chemotherapy are the cornerstone in NPC treatment. Further check the potential synergistic of DC with radiation therapy and chemotherapy will increase the value of research. According to the ROS data (Fig. S1), DC treatment did not increase ROS production. Therefore, DC induces DNA damage and then causes apoptosis. In this study, our results suggested that DC induces G2/M cell cycle arrest. Previous studies have shown that DNA damage cues activate the sensory DNA-PK/ATM/ATR kinases (65,66), which relay inhibits progression into mitosis and involves phosphorylation of p53 (67,68) that ultimately serve to inactivate the cyclin B-cdc2 complex. Therefore, ATM/ATR and p53 may be potential targets of DC.

In conclusion, the study results showed that DC inhibited the proliferation of human NPC cells through induced DNA damage, caused an increase in death receptor expression and mitochondrial membrane depolarization, adjustment of the MAPK pathway, induction of cell cycle arrest and apoptosis. Notably, this is the first anti-nasopharyngeal cancer study on the natural Chinese herbal medicine β-hydrocarbon alkaloid DC against NPC. The lack of *in vivo* experiments was a potential limitation to the present study. However, many published article have suggested the antitumor functions and its biological relevance of pure compounds in nasopharyngeal carcinoma *in vitro* and *in vivo* (69-71). These *in vivo* study groups received a daily intraperitoneal injection in animal model, therefore, it can eliminate the problem of poor bioavailability of natural compounds. We deduce that DC may be a promising anticancer drug.

Acknowledgements

Not applicable.

Funding

This study was supported by grants from National Science Council, Taiwan (grant no. MOST 109-2314-B-371-005) and Changhua Christian Hospital (grant no. 109-CCH-MST-161).

Availability of data and materials

All data generated or analyzed during this study are included in this published article.

Authors' contributions

MCH, MJH and JTL conceptualized and designed the study. CCL, YCC, YSL and HYH. acquired, analyzed and interpreted the data. MCH, CCL and MJH drafted and revised the manuscript. MJH and JTL had overall responsibility for the published work. MJH and CCL confirm the authenticity of all the raw data. All authors read and approved the final manuscript.

Ethics approval and consent to participate

Not applicable.

Patient consent for publication

Not applicable.

Competing interests

The authors declare that they have no competing interests.

References

1. Du T, Xiao J, Qiu Z and Wu K: The effectiveness of intensity-modulated radiation therapy versus 2D-RT for the treatment of nasopharyngeal carcinoma: A systematic review and meta-analysis. PLoS One 14: e0219611, 2019.
2. Chen YP, Chan AT, Le QT, Blanchard P, Sun Y and Ma J: Nasopharyngeal carcinoma. Lancet 394: 64-80, 2019.
3. Chan KC, Woo JK, King A, Zee BC, Lam WK, Chan SL, Chu SW, Mak C, Tse IO, Leung SY, *et al*: Analysis of plasma Epstein-Barr virus DNA to screen for nasopharyngeal cancer. N Engl J Med 377: 513-522, 2017.
4. Tsang RK: Nasopharyngeal carcinoma-improving cure with technology and clinical trials. World J Otorhinolaryngol Head Neck Surg 6: 1-3, 2020.
5. Sun XS, Li XY, Chen QY, Tang LQ and Mai HQ: Future of radiotherapy in nasopharyngeal carcinoma. Br J Radiol 92: 20190209, 2019.
6. Guo SS, Hu W, Chen QY, Li JM, Zhu SH, He Y, Li JW, Xia L, Ji L, Lin CY, *et al*: Pretreatment quality of life as a predictor of survival for patients with nasopharyngeal carcinoma treated with IMRT. BMC Cancer 18: 114, 2018.
7. Liu LT, Liang YJ, Guo SS, Mo HY, Guo L, Wen YF, Xie HJ, Tang QN, Sun XS, Liu SL, *et al*: Induction chemotherapy followed by radiotherapy versus concurrent chemoradiotherapy in the treatment of different risk locoregionally advanced nasopharyngeal carcinoma. Ther Adv Med Oncol 12: 1758835920928214, 2020.
8. Zhao WY, Shang XY, Zhao L, Yao GD, Sun Z, Huang XX and Song SJ: Bioactivity-guided isolation of β-carboline alkaloids with potential anti-hepatoma effect from *Picrasma quassioides* (D. Don) Benn. Fitoterapia 130: 66-72, 2018.
9. Lee HE, Choi ES, Shin JA, Kim LH, Cho NP and Cho SD: Apoptotic effect of methanol extract of *Picrasma quassioides* by regulating specificity protein 1 in human cervical cancer cells. Cell Biochem Funct 32: 229-235, 2014.
10. Xie DP, Gong YX, Jin YH, Ren CX, Liu Y, Han YH, Jin MH, Zhu D, Pan QZ, Yu LY, *et al*: Anti-tumor properties of *Picrasma quassioides* extracts in H-Ras^{G12V} liver cancer are mediated through ROS-dependent mitochondrial dysfunction. nticancer Res 40: 3819-3830, 2020.
11. Shin NR, Shin IS, Jeon CM, Hong JM, Oh SR, Hahn KW and Ahn KS: Inhibitory effects of *Picrasma quassioides* (D.Don) Benn. On airway inflammation in a murine model of allergic asthma. Mol Med Rep 10: 1495-1500, 2014.

12. Ma Y and Wink M: The beta-carboline alkaloid harmine inhibits BCRP and can reverse resistance to the anticancer drugs mitoxantrone and camptothecin in breast cancer cells. Phytother Res 24: 146-149, 2010.
13. Zhao F, Tang Q, Xu J, Wang S, Li S, Zou X and Cao Z: Dehydrocrenatidine inhibits voltage-gated sodium channels and ameliorates mechanic allodia in a rat model of neuropathic pain. Toxins (Basel) 11: 229, 2019.
14. Zhao WY, Chen JJ, Zou CX, Zhou WY, Yao GD, Wang XB, Lin B, Huang XX and Song SJ: Effects of enantiomerically Pure β-carboline alkaloids from *Picrasma quassioides* on human hepatoma cells. Planta Med 85: 648-656, 2019.
15. Zhao F, Gao Z, Jiao W, Chen L, Chen L and Yao X: In vitro anti-inflammatory effects of beta-carboline alkaloids, isolated from *Picrasma quassioides*, through inhibition of the iNOS pathway. Planta Med 78: 1906-1911, 2012.
16. Jiao WH, Chen GD, Gao H, Li J, Gu BB, Xu TT, Yu HB, Shi GH, Yang F, Yao XS and Lin HW: (±)-Quassidines I and J, two pairs of cytotoxic bis-β-carboline alkaloid enantiomers from *Picrasma quassioides*. J Nat Prod 78: 125-130, 2015.
17. Gong YX, Liu Y, Jin YH, Jin MH, Han YH, Li J, Shen GN, Xie DP, Ren CX, Yu LY, *et al*: *Picrasma quassioides* extract elevates the cervical cancer cell apoptosis through ROS-mitochondrial axis activated p38 MAPK signaling pathway. In Vivo 34: 1823-1833, 2020.
18. Zhang J, Zhu N, Du Y, Bai Q, Chen X, Nan J, Qin X, Zhang X, Hou J, Wang Q and Yang J: Dehydrocrenatidine is a novel janus kinase inhibitor. Mol Pharmacol 87: 572-581, 2015.
19. Liao SK, Perng YP, Shen YC, Chung PJ, Chang YS and Wang CH: Chromosomal abnormalities of a new nasopharyngeal carcinoma cell line (NPC-BM1) derived from a bone marrow metastatic lesion. Cancer Genet Cytogenet 103: 52-58, 1998.
20. Liu YT, Chuang YC, Lo YS, Lin CC, His YT, Hsieh MJ and Chen MK: Asiatic acid, extracted from centella asiatica and induces apoptosis pathway through the phosphorylation p38 mitogen-activated protein kinase in cisplatin-resistant nasopharyngeal carcinoma cells. Biomolecules 10: 184, 2020.
21. Jana A, Das A, Krett NL, Guzman G, Thomas A, Mancinelli G, Bauer J, Ushio-Fukai M, Fukai T and Jung B: Nuclear translocation of Atox1 potentiates activin A-induced cell migration and colony formation in colon cancer. PLoS One 15: e0227916, 2020.
22. Chen YT, Hsieh MJ, Chen PN, Weng CJ, Yang SF and Lin CW: Erianin induces apoptosis and autophagy in oral squamous cell carcinoma cells. Am J Chin Med 48: 183-200, 2020.
23. Hsieh MY, Hsieh MJ, Lo YS, Lin CC, Chuang YC, Chen MK and Chou MC: Modulating effect of coronarin D in 5-fluorouracil resistance human oral cancer cell lines induced apoptosis and cell cycle arrest through JNK1/2 signaling pathway. Biomed Pharmacother 128: 110318, 2020.
24. Tunc D, Dere E, Karakas D, Cevatemre B, Yilmaz VT and Ulukaya E: Cytotoxic and apoptotic effects of the combination of palladium (II) 5,5-diethylbarbiturate complex with bis(2-pyridylmethyl)amine and curcumin on non small lung cancer cell lines. Bioorg Med Chem 25: 1717-1723, 2017.
25. Zhao L, Fong AH, Liu N and Cho WC: Molecular subtyping of nasopharyngeal carcinoma (NPC) and a microRNA-based prognostic model for distant metastasis. J Biomed Sci 25: 16, 2018.
26. Sun PY, Chen YH, Feng XB, Yang CX, Wu F and Wang RS: High-dose static and dynamic intensity-modulated radiotherapy combined with chemotherapy for patients with locally advanced nasopharyngeal carcinoma improves survival and reduces brainstem toxicity. Med Sci Monit 24: 8849-8859, 2018.
27. Wang F, Jiang C, Wang L, Yan F, Sun Q, Ye Z, Liu T, Fu Z and Jiang Y: Influence of concurrent chemotherapy on locoregionally advanced nasopharyngeal carcinoma treated with neoadjuvant chemotherapy plus intensity-modulated radiotherapy: A retrospective matched analysis. Sci Rep 10: 2489, 2020.
28. Zheng ZQ, Li ZX, Zhou GQ, Lin L, Zhang LL, Lv JW, Huang XD, Liu RQ, Chen F, He XJ, *et al*: Long noncoding RNA FAM225A promotes nasopharyngeal carcinoma tumorigenesis and metastasis by acting as ceRNA to sponge miR-590-3p/miR-1275 and upregulate ITGB3. Cancer Res 79: 4612-4626, 2019.
29. Jain CK, Majumder HK and Roychoudhury S: Natural compounds as anticancer agents targeting DNA topoisomerases. Curr Genomics 18: 75-92, 2017.
30. Cao R, Peng W, Wang Z and Xu A: beta-Carboline alkaloids: Biochemical and pharmacological functions. Curr Med Chem 14: 479-500, 2007.
31. Mansoor TA, Ramalho RM, Mulhovo S, Rodrigues CM and Ferreira MJ: Induction of apoptosis in HuH-7 cancer cells by monoterpene and beta-carboline indole alkaloids isolated from the leaves of tabernaemontana elegans. Bioorg Med Chem Lett 19: 4255-4258, 2009.
32. Bemis DL, Capodice JL, Gorroochurn P, Katz AE and Buttyan R: Anti-prostate cancer activity of a beta-carboline alkaloid enriched extract from rauwolfia vomitoria. Int J Oncol 29: 1065-1073, 2006.
33. Bai J, Li Y and Zhang G: Cell cycle regulation and anticancer drug discovery. Cancer Biol Med 14: 348-362, 2017.
34. Yam CH, Fung TK and Poon RY: Cyclin A in cell cycle control and cancer. Cell Mol Life Sci 59: 1317-1326, 2002.
35. Vigneron S, Sundermann L, Labbé JC, Pintard L, Radulescu O, Castro A and Lorca T: Cyclin A-cdk1-dependent phosphorylation of bora is the triggering factor promoting mitotic entry. Dev Cell 45: 637-650.e7, 2018.
36. Sun X, Zhangyuan G, Shi L, Wang Y, Sun B and Ding Q: Prognostic and clinicopathological significance of cyclin B expression in patients with breast cancer: A meta-analysis. Medicine (Baltimore) 96: e6860, 2017.
37. Ujiki MB, Ding XZ, Salabat MR, Bentrem DJ, Golkar L, Milam B, Talamonti MS, Bell RH Jr, Iwamura T and Adrian TE: Apigenin inhibits pancreatic cancer cell proliferation through G2/M cell cycle arrest. Mol Cancer 5: 76, 2006.
38. Pomerening JR, Kim SY and Ferrell JE Jr: Systems-level dissection of the cell-cycle oscillator: Bypassing positive feedback produces damped oscillations. Cell 122: 565-578, 2005.
39. Sha W, Moore J, Chen K, Lassaletta AD, Yi CS, Tyson JJ and Sible JC: Hysteresis drives cell-cycle transitions in xenopus laevis egg extracts. Proc Natl Acad Sci USA 100: 975-980, 2003.
40. Mota NSRS, Kviecinski MR, Felipe KB, Grinevicius VMAS, Siminski T, Almeida GM, Zeferino RC, Pich CT, Filho DW and Pedrosa RC: β-carboline alkaloid harmine induces DNA damage and triggers apoptosis by a mitochondrial pathway: Study in silico, in vitro and in vivo. Int J Funct Nutr 1: 1, 2020.
41. Johnson J, Thijssen B, McDermott U, Garnett M, Wessels LF and Bernards R: Targeting the RB-E2F pathway in breast cancer. Oncogene 35: 4829-4835, 2016.
42. Ahmad I, Fakhri S, Khan H, Jeandet P, Aschner M and Yu ZL: Targeting cell cycle by β-carboline alkaloids in vitro: Novel therapeutic prospects for the treatment of cancer. Chem Biol Interact 330: 109229, 2020.
43. Cao MR, Li Q, Liu ZL, Liu HH, Wang W, Liao XL, Pan YL and Jiang JW: Harmine induces apoptosis in HepG2 cells via mitochondrial signaling pathway. Hepatobiliary Pancreat Dis Int 10: 599-604, 2011.
44. Abdelsalam MA, AboulWafa OM, Badawey EA, El-Shoukrofy MS, El-Miligy MM and Gouda N: Design and synthesis of some β-carboline derivatives as multi-target anticancer agents. Future Med Chem 10: 2791-2814, 2018.
45. Portt L, Norman G, Clapp C, Greenwood M and Greenwood MT: Anti-apoptosis and cell survival: A review. Biochim Biophys Acta 1813: 238-259, 2011.
46. Ouyang L, Shi Z, Zhao S, Wang FT, Zhou TT, Liu B and Bao JK: Programmed cell death pathways in cancer: A review of apoptosis, autophagy and programmed necrosis. Cell Prolif 45: 487-498, 2012.
47. Wang S and El-Deiry WS: TRAIL and apoptosis induction by TNF-family death receptors. Oncogene 22: 8628-8633, 2003.
48. Elrod HA and Sun SY: Modulation of death receptors by cancer therapeutic agents. Cancer Biol Ther 7: 163-173, 2008.
49. Kischkel FC, Lawrence DA, Chuntharapai A, Schow P, Kim KJ and Ashkenazi A: Apo2L/TRAIL-dependent recruitment of endogenous FADD and caspase-8 to death receptors 4 and 5. Immunity 12: 611-620, 2000.
50. Lin Y, Devin A, Rodriguez Y and Liu ZG: Cleavage of the death domain kinase RIP by caspase-8 prompts TNF-induced apoptosis. Genes Dev 13: 2514-2526, 1999.
51. Deng Z, Gao P, Yu L, Ma B, You Y, Chan L, Mei C and Chen T: Ruthenium complexes with phenylterpyridine derivatives target cell membrane and trigger death receptors-mediated apoptosis in cancer cells. Biomaterials 129: 111-126, 2017.
52. Derakhshan A, Chen Z and Van Waes C: Therapeutic small molecules target inhibitor of apoptosis proteins in cancers with deregulation of extrinsic and intrinsic cell death pathways. Clin Cancer Res 23: 1379-1387, 2017.
53. Han NN, Zhou Q, Huang Q and Liu KJ: Carnosic acid cooperates with tamoxifen to induce apoptosis associated with caspase-3 activation in breast cancer cells in vitro and in vivo. Biomed Pharmacother 89: 827-837, 2017.

54. Debatin KM: Apoptosis pathways in cancer and cancer therapy. Cancer Immunol Immunother 53: 153-159, 2004.
55. Li-Weber M: Targeting apoptosis pathways in cancer by Chinese medicine. Cancer Lett 332: 304-312, 2013.
56. Li C, Wang Y, Wang C, Yi X, Li M and He X: Anticancer activities of harmine by inducing a pro-death autophagy and apoptosis in human gastric cancer cells. Phytomedicine 28: 10-18, 2017.
57. Hamsa TP and Kuttan G: Harmine activates intrinsic and extrinsic pathways of apoptosis in B16F-10 melanoma. Chin Med 6: 11, 2011.
58. Zaid H, Silbermann M, Amash A, Gincel D, Abdel-Sattar E and Sarikahya NB: Medicinal plants and natural active compounds for cancer chemoprevention/chemotherapy. Evid Based Complement Alternat Med 2017: 7952417, 2017.
59. Zhang P, Huang CR, Wang W, Zhang XK, Chen JJ, Wang JJ, Lin C and Jiang JW: Harmine hydrochloride triggers G2 phase arrest and apoptosis in MGC-803 cells and SMMC-7721 cells by upregulating p21, activating caspase-8/Bid, and downregulating ERK/bad pathway. Phytother Res 30: 31-40, 2016.
60. Yue J and López JM: Understanding MAPK signaling pathways in apoptosis. Int J Mol Sci 21: 2346, 2020.
61. Junttila MR, Li SP and Westermarck J: Phosphatase-mediated crosstalk between MAPK signaling pathways in the regulation of cell survival. FASEB J 22: 954-965, 2008.
62. Fan Y, Patima A, Chen Y, Zeng F, He W, Luo L, Jie Y, Zhu Y, Zhang L, Lei J, *et al*: Cytotoxic effects of β-carboline alkaloids on human gastric cancer SGC-7901 cells. Int J Clin Exp Med 8: 12977-12982, 2015.
63. Chien CC, Wu MS, Shen SC, Ko CH, Chen CH, Yang LL and Chen YC: Activation of JNK contributes to evodiamine-induced apoptosis and G2/M arrest in human colorectal carcinoma cells: A structure-activity study of evodiamine. PLoS One 9: e99729, 2014.
64. Lee YJ, Choi SY and Yang JH: NMDA receptor-mediated ERK 1/2 pathway is involved in PFHxS-induced apoptosis of PC12 cells. Sci Total Environ 491-492: 227-234, 2014.
65. Al-Ejeh F, Kumar R, Wiegmans A, Lakhani SR, Brown MP and Khanna KK: Harnessing the complexity of DNA-damage response pathways to improve cancer treatment outcomes. Oncogene 29: 6085-6098, 2010.
66. Boutros R, Lobjois V and Ducommun B: CDC25 phosphatases in cancer cells: Key players? Good targets? Nat Rev Cancer 7: 495-507, 2007.
67. Freed-Pastor WA, Mizuno H, Zhao X, Langerød A, Moon SH, Rodriguez-Barrueco R, Barsotti A, Chicas A, Li W, Polotskaia A, *et al*: Mutant p53 disrupts mammary tissue architecture via the mevalonate pathway. Cell 148: 244-258, 2012.
68. Freed-Pastor WA and Prives C: Mutant p53: One name, many proteins. Genes Dev 26: 1268-1286, 2012.
69. Fang EF, Zhang CZ, Ng TB, Wong JH, Pan WL, Ye XJ, Chan YS and Fong WP: Momordica Charantia lectin, a type II ribosome inactivating protein, exhibits antitumor activity toward human nasopharyngeal carcinoma cells in vitro and in vivo. Cancer Prev Res (Phila) 5: 109-121, 2012.
70. Song Y, Yang J, Bai WL and Ji WY: Antitumor and immunoregulatory effects of astragalus on nasopharyngeal carcinoma in vivo and in vitro. Phytother Res 25: 909-915, 2011.
71. Zeng M, Wu X, Li F, She W, Zhou L, Pi B, Xu Z and Huang X: Laminaria japonica polysaccharides effectively inhibited the growth of nasopharyngeal carcinoma cells in vivo and in vitro study. Exp Toxicol Pathol 69: 527-532, 2017.